ARTICLE

High-Throughput Screening Platform for Engineered Nanoparticle-Mediated Genotoxicity Using CometChip Technology

Christa Watson,[†] Jing Ge,[‡] Joel Cohen,[†] Georgios Pyrgiotakis,[†] Bevin P. Engelward,[‡,§,*] and Philip Demokritou[†,§,*]

[†]Department of Environmental Health, Center for Nanotechnology and Nanotoxicology, Harvard School of Public Health, Boston, Massachusetts 02115, United States and [‡]Department of Biological Engineering, Massachusetts Institute of Technology, Cambridge, Massachusetts 02139, United States. [§]These authors contributed equally to this work.

ABSTRACT

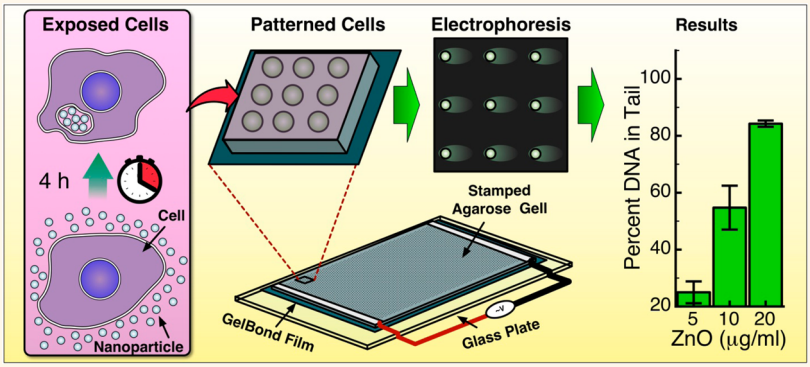

The likelihood of intentional and unintentional engineered nanoparticle (ENP) exposure has dramatically increased due to the use of nanoenabled products. Indeed, ENPs have been incorporated in many useful products and have enhanced our way of life. However, there are many unanswered questions about the consequences of nanoparticle exposures, in particular, with regard to their potential to damage the genome and thus potentially promote cancer. In this study, we present a high-throughput screening assay based upon the recently developed CometChip technology, which enables evaluation of single-stranded DNA breaks, abasic sites, and alkali-sensitive sites in cells exposed to ENPs. The strategic microfabricated, 96-well design and automated processing improves efficiency, reduces processing time, and suppresses user bias in comparison to the standard comet assay. We evaluated the versatility of this assay by screening five industrially relevant ENP exposures (SiO_2, ZnO, Fe_2O_3, Ag, and CeO_2) on both suspension human lymphoblastoid (TK6) and adherent Chinese hamster ovary (H9T3) cell lines. MTT and CyQuant NF assays were employed to assess cellular viability and proliferation after ENP exposure. Exposure to ENPs at a dose range of 5, 10, and 20 μg/mL induced dose-dependent increases in DNA damage and cytotoxicity. Genotoxicity profiles of ZnO > Ag > Fe_2O_3 > CeO_2 > SiO_2 in TK6 cells at 4 h and Ag > Fe_2O_3 > ZnO > CeO_2 > SiO_2 in H9T3 cells at 24 h were observed. The presented CometChip platform enabled efficient and reliable measurement of ENP-mediated DNA damage, therefore demonstrating the efficacy of this powerful tool in nanogenotoxicity studies.

KEYWORDS: nanotoxicology · genotoxicity · comet · DNA damage · CometChip · engineered nanoparticles

The advent of nanotechnology has produced novel forms of engineered nanoparticles (ENPs), which have broad utility in numerous nanoenabled commercial products. In fact, according to the Woodrow Wilson Center Project for Emerging Nanotechnologies, the amount of nanoenabled consumer products available commercially has risen by ~500% since 2006.[1] Increased availability and use of nanoenabled products such as cosmetics, sunscreens,[2] and toner formulations[3] has potentially contributed to unintentional exposures experienced by adults and children.[4,5] Likewise, the probability of intentional exposures has grown due to the

* Address correspondence to pdemokri@hsph.harvard.edu, bevin@mit.edu.

Received for review September 17, 2013 and accepted February 16, 2014.

Published online March 11, 2014
10.1021/nn404871p

development of nanoenabled drug delivery systems, diagnostic tools, or cancer therapies that bring promise to revolutionize the medical field.[6]

Although the applications and benefits of ENPs appear limitless, there is growing concern about the consequences of ENP exposures.[7−10] Several studies have indicated that exposure to ENPs via inhalation, dermal, or oral routes can pose adverse health effects.[11,12] A well-known paradigm of metal or metal oxide ENP toxicity is the production of reactive oxygen species (ROS), which can overwhelm innate antioxidants, thereby producing oxidative stress.[13,14] Oxidative stress can in turn lead to the formation of a wide range of DNA lesions, many of which can be either cytotoxic or mutagenic.[15] Thus, there is an established link between excess oxidative stress and associated DNA damage, aging, and the increased risk of cancer.[16−18] However, despite the importance of nanoparticle exposure-induced DNA damage as a potential cancer risk factor, relatively few studies have focused on the DNA-damaging potential of ENPs. This knowledge gap has been largely driven by the fact that existing ENP genotoxicity *in vitro* cellular assays are not equipped to undertake the vast libraries of ENPs that currently exist or are being developed.

Presently, the genotoxicity assays that are employed for ENP assessments are adaptations of chemical genotoxic assays such as the Ames test, *in vitro* micronucleus, and the single-cell electrophoresis or comet assays. For example, Li and co-authors utilized the Ames test along with the *in vitro* micronucleus assay (measurement of double-strand breaks/aneuploidy) to evaluate the mutagenic and genotoxic potential of 5 nm silver nanoparticles, respectively.[19] Within that study, the authors found that the Ames test was not as sensitive as the micronucleus assay when evaluating the genotoxicity of silver ENPs in TK6 cells. The decreased sensitivity of the Ames test, which uses bacterial cells to assess mutagenicity, may be attributed to the fact that bacterial cells are not endocytic, suggesting that the Ames test is not suitable for the evaluation of certain nanoparticles.[20,21] The micronucleus assay has also been utilized in many studies to assess nanoparticle-mediated chromosomal damage.[22−25] However, the assay has been found to be problematic due to issues with reagent interference (*i.e.*, cytochalasin B) with cellular uptake of nanoparticles, thus generating false negatives.[26,27] Other assays such as the 8-oxoguanine (8-oxo-dG) ELISA have been employed to measure nanoparticle-mediated DNA damage.[28] Although high-throughput can be achieved with the 96-well plate design, this assay only measures 8-oxo-dG, a biomarker of DNA oxidation, and does not provide information on other classes of DNA damage (*e.g.*, double- and single-strand breaks, abasic sites, and alkali-sensitive sites), which can be detected using the comet assay.

The most widely used assay for evaluating DNA damage associated with ENP exposures is the comet assay.[29] Briefly, the underlying principle of the comet assay is that, during electrophoresis, damaged DNA migrates more readily in an agarose matrix than undamaged DNA. The comet-like structures that are formed during this process are fluorescently stained, and imaging software is used for quantitative analysis to determine the amount of DNA damage on a cell-by-cell basis.[30,31] However, similar to the aforementioned genotoxicity assays, issues with nanoparticle interference have been reported with traditional comet assay efficacy. Stone *et al.* suggested that artifacts could occur when residual nanoparticles interacted with naked DNA after cell lysis, thus generating "artificial" damage.[32] Yet, in a recent investigation, where studies were conducted to evaluate the level of strand breaks induced by close proximity nanoparticles *versus* whole cell exposures, such issues of nanoparticle interferences with the comet assay were disproven.[33]

While the comet assay has been found to be effective in assaying ENPs, the technique suffers from low-throughput and poor reproducibility, due in part to sample-to-sample variation (*e.g.*, different results for the same sample when analyzed on two separate glass slides).[34] These inherent issues make the comet assay inefficient in conducting comprehensive investigations that are needed for assessing not only multiple ENPs but also multiple parameters such as size, charge, and shape. Thus, there is a significant need for a high-throughput screening tool for assessing ENP-mediated DNA damage.[35]

Here we describe an efficient screening platform for assessing DNA damage associated with ENP exposures. Our approach is based upon the CometChip, developed in the laboratories of Bevin Engleward and Sangeeta Bhatia,[36,37] which uses microfabrication technology to create a microarray of precisely ordered microwells within a bed of agarose, each with an adjustable diameter as small as a single cell. Ultimately, we have created a more effective and high-throughput platform, which could help to overcome current limitations in our ability to assess the vast libraries of new and existing ENPs and would thus reduce potentially serious public health issues associated with ENP-induced genotoxicity. Such a rapid screening assay can also be pivotal in our quest for developing safer-by-design nanomaterials[38] and help in understanding the structure−activity relationships in terms of genotoxicity.

RESULTS AND DISCUSSION

Characterization of ENP Powders. To explore the utility of the CometChip platform and to learn about the genotoxic potential of ENPs, we elected to study a variety of industrially relevant ENPs, including

TABLE 1. Physicochemical Characterization of ENPs Used in DNA Damage Assessments[a]

				DI H_2O			MEM/10%FBS			RPMI/10%HS		
material	SSA (cm^2)	d_{BET} (nm)	d_{XRD} (nm)	d_H (nm)	PDI	ζ (mV)	d_H (nm)	PDI	ζ (mV)	d_H (nm)	PDI	ζ (mV)
SiO_2	154	14.7	NA	214 ± 4	0.324	−22 ± 1	227 ± 43	0.402	−21 ± 3.0	252 ± 16.1	0.372	−25.1 ± 3.2
CeO_2	206	4.03	11.5	348 ± 8	0.270	−20 ± 1	277 ± 30	0.275	−21 ± 2.2	236 ± 3.7	0.294	−25.2 ± 7.1
ZnO	17.7	60.5	20	225 ± 24	0.224	19.1 ± 2.2	327 ± 71	0.232	−13.3 ± 2.4	232 ± 3.7	0.128	−12.4 ± 0.9
Ag	13.7	41.8	35	211 ± 68	0.399	−28 ± 0.9	179 ± 3	0.290	−11.5 ± 1.7	189 ± 3.1	0.290	−9.8 ± 0.83
Fe_2O_3	58.1	19.7	31.1	1444 ± 235	0.258	−28 ± 0.6	934 ± 158	0.459	−10.9 ± 0.28	1231 ± 173	0.477	−8.11 ± 2.1

[a] SSA (specific surface area), by nitrogen adsorption/Brunauer−Emmett−Teller (BET) method; d_{BET}, primary particle diameter determined from SSA; d_{XRD}, particle diameter as determined by X-ray diffraction; d_H, hydrodynamic diameter determined by DLS; PDI, polydispersity index measured by DLS; ζ, zeta-potential measured by DLS.

amorphous silica (SiO_2), silver (Ag), iron oxide (Fe_2O_3), zinc oxide (ZnO), and cerium oxide (CeO_2). These particular ENPs were selected in part because they are currently under investigation by the Organization for Economic Cooperation and Development (OECD) but also because they are widely used in many nanoenabled products.[39] The panel of industrially relevant ENPs was synthesized in-house using the flame spray pyrolysis based Harvard VENGES system.[40,41] Each ENP underwent detailed physicochemical and morphological characterization in powder form including Brunauer−Emmett−Teller (d_{BET}) to determine the specific surface area (SSA) and particle crystal diameter (d_{XRD}) using X-ray diffraction (Table 1) (see Methods section for details). As shown in Table 1, the primary particle size of the ENPs is in the nanoscale. The TEM images provided in Supporting Information Figure S1 depict ENP aggregates (distinguished by their fractal geometry and sinter necks) as well as agglomerates (particle units composed of several aggregates that might be formed due to van der Waals forces encountered during particle suspension in ethanol for TEM grid sample preparation). The ENPs in nanopowder form appeared to form chain-like aggregates, typical of metal oxides generated in a flame pyrolysis process (Figure S1).[42] More specifically, silver and cerium ENPs resembled more spherical morphologies, whereas iron oxide ENPs had more of a hexagonal shape. Zinc oxide ENPs utilized in this study were rod-shaped, and silica was without a definitive shape, thus amorphous.

Dispersion and Characterization of ENP Suspensions. The measured properties of ENP suspensions (hydrodynamic diameter (d_H), polydispersity index (PDI), zeta-potential (ζ), and specific conductance (σ), in DI H_2O and the cell culture media are summarized in Table 1. In general, most ENPs utilized in this study formed fairly monodisperse suspensions (PDI < 0.4) of agglomerates ranging from 200−400 nm in diameter in DI H_2O and media containing serum. Fe_2O_3 formed larger agglomerates and slightly higher PDI values of 0.459 and 0.477 in MEM and RPMI containing serum, respectively, likely attributable to interparticle magnetic forces common to this material at similar primary particle size.[43,44] These values are similar to values previously measured for similar metal oxide ENPs.[45]

Development of a High-Throughput ENP Genotoxicity Screening Assay Using the CometChip Technology. The following steps were performed as part of the development of the assay.

Microfabrication of a Microwell Array. Patterned arrays of microwells were created using a silicon stamp which consists of micrometer-scale posts (Figure 1A). The microposts, created by photolithography, have a tunable diameter, ranging from ~10 to 50 μm, in order to accommodate different-sized cells.[36] The microfabricated stamp is placed into molten agarose, which is applied to a sheet of GelBond film, then allowed to solidify to create a bed of microwells once the stamp is removed. A bottomless 96-well plate is then pressed onto the surface of microwells to create 96 macrowells, each of which has 200−300 microwells on its bottom surface (Figure 1A). Cells are captured in the microwells to create an array of cells embedded in agarose (Figure 1D), which can then be processed using the same methods as the traditional comet assay (*e.g.*, lysis and electrophoresis). For the purposes of the studies presented here, we created microwells with 40 μm diameters that are effective for capture of nonadherent TK6 cells and adherent cell line H9T3.

Throughput is a major limitation for the traditional comet assay, wherein for each condition or exposure, treated cell suspensions are embedded in low melting point agarose and placed on a glass slide. Glass slides are awkward to handle, thus limiting the number of samples that can be run in parallel, introducing significant experimental noise between samples.[46] The microfabrication approach of the CometChip enables analysis of 96 samples in parallel, which greatly reduces labor and also suppresses variation due to sample handling.[37]

ENP Suspension Preparation and Cell Exposure. ENP suspensions were prepared according to a protocol developed in our group (Figure 1B) (see Methods for details). Briefly, ENPs are sonicated in deionized water to ensure dissociation of agglomerates and subsequently added to cell culture media. ENPs in media are then combined with cell suspensions or monolayers and incubated for

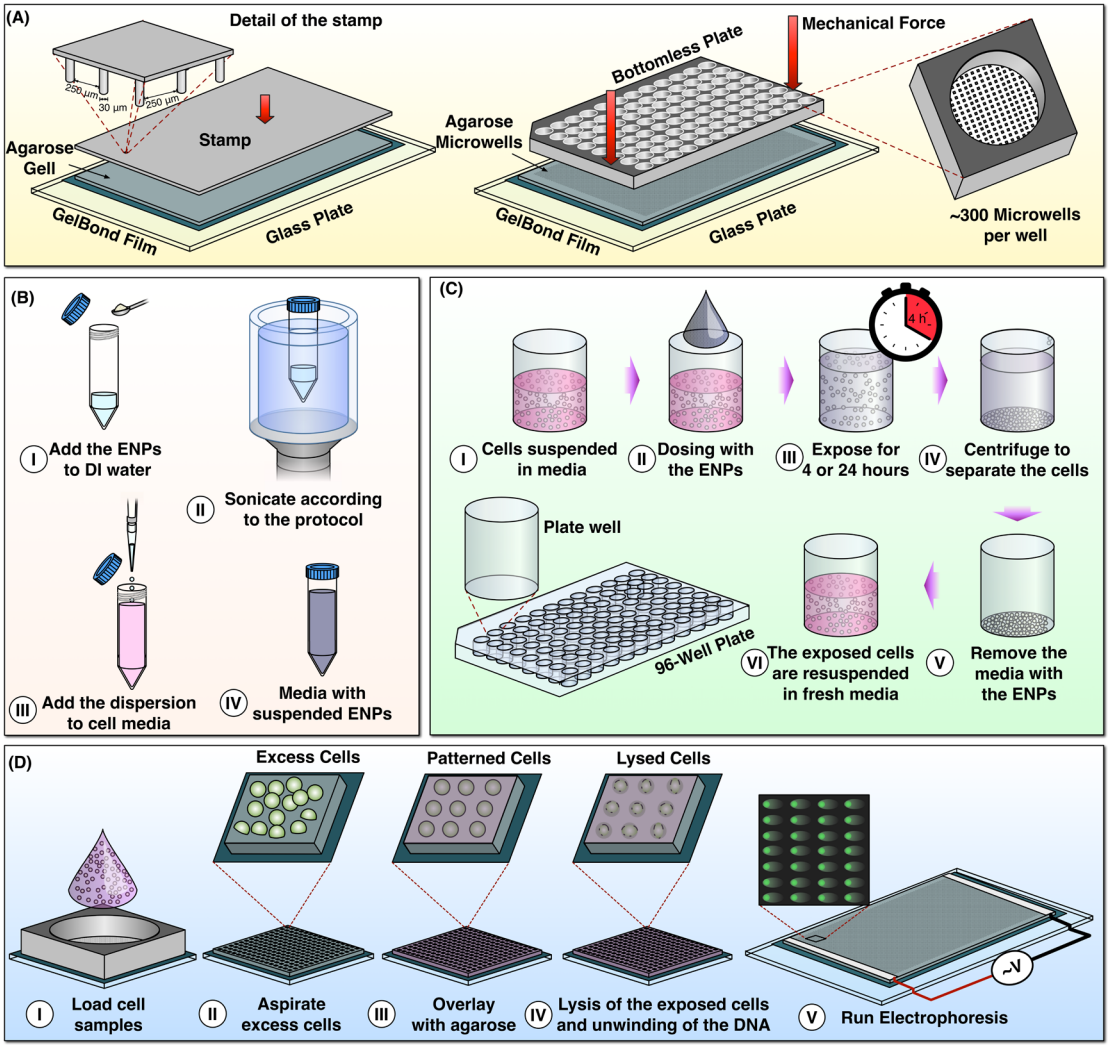

Figure 1. Protocol for the CometChip (A) assembly of macrowell comet array. Agarose gel containing microwells is situated on GelBond film sandwiched between a glass substrate and a bottomless 96-well plate, which is then sealed with mechanical force. Approximately 300 arrayed microwells comprise the bottom of each macrowell. (B) Preparation of the nanoparticle suspension according to the protocol by Cohen *et al.* (C) Protocol for exposing the cells to the nanoparticles. (D) Loading of the exposed cell samples in the macrowells and running the microwell assay.

4 or 24 h prior to loading the cells onto the CometChip for DNA damage analysis. After exposure, cells are separated from nanoparticle suspensions by centrifugation and aspiration. Trypsin is added to adherent cells to produce treated cell suspensions. Suspension cells are then simply added to the macrowells of the CometChip for cell loading into the arrayed microwells.

Agarose Encapsulation of Exposed Cells and Electrophoresis. To study genotoxicity, log phase cells were exposed to ENPs and loaded into the microwells by gravitational settling. After 30 min, most of the microwells contain cells (Figure 1D) and excess media/cells can be aspirated. Residual cells and ENPs are rinsed from macrowells and agarose using three gentle washes of warm phosphate buffered saline. To prevent cells from being displaced during handling, a thin layer of low melting point molten agarose is used to secure cells within their microwells. Subsequently, the arrayed cells are processed using conditions that are similar to the traditional assay. Briefly, cells are lysed in a strong surfactant and alkaline solution for 24 h at 4 °C and then subjected to electrophoresis, which causes relaxed loops and fragments of DNA to migrate through the agarose gel.

Comet Imaging. Due to the format of the CometChip, 96 ENP conditions can be readily imaged and analyzed in parallel. In the traditional comet assay, imaging and/or scoring 96 samples is arduous and time-consuming due to possible sparse areas or clumped comets.[47] Traditionally, the user is required to scan each treatment or slide to detect usable comets, which can be prone to bias. Obtaining quantitative data from the customized CometChip system is simplified by exploiting the array format, which prevents overlap and bias and also enables maximization of the number of comets per unit area. Images are collected using a standard fluorescent microscope Nikon 80i upright microscope coupled with an automatic scanning stage

(ProScan II, Prior Scientific). The microfabrication approach used to create the microwell array offers an additional significant advantage during imaging. Specifically, treated cells and subsequent comets are located on one focal plane, which prevents the need to adjust focus for each comet and thus enables multiple comets to be captured in focus in a single image, reducing imaging time significantly. In addition to faster data collection, the CometChip approach also increases throughput *via* automated data analysis. In the traditional comet assay, for each condition, ~100 independent comets need to be analyzed one-by-one for every condition using a computer software program, which is very time-consuming. For the CometChip, the fabricated microwells provide consistent or fixed comet head size using custom software, which simplifies the identification of head/tail transitions enabling accurate comet analysis. Furthermore, the custom software is designed to select and analyze comets that lie specifically within the coded array and excludes cells off the array that potentially have overlapped. With imaging reduced to fewer than 10 images per condition and analysis done in batch form using custom software, the speed of data collection and analysis is orders of magnitude faster than the traditional assay.[36]

Assessing Nanoparticle-Mediated DNA Damage Using the Proposed CometChip Platform. To explore the versatility and sensitivity of the CometChip platform, we performed simultaneous DNA damage assessments of our ENP panel using three concentrations (5, 10, 20 μg/mL) and two cell lines, suspension (TK6) and adherent (H9T3). The selected dose range of 5, 10, and 20 μg/mL was determined to be lower than a predetermined IC_{50} value of 25 μg/mL in the majority of the ENP panel (data not shown). Human lymphoblastoid cells (TK6) and Chinese hamster ovary cells were utilized in our assessments as they have been historically used for genotoxicity evaluations and are the most commonly used cell lines when performing the comet assay.[48,49] It is worth noting that the selected cell lines are used not as a specific route of exposure or physiological relevance, but rather to demonstrate the applicability of the developed CometChip approach on the use of both suspended and adherent cell lines.

In evaluating the DNA damage induced by ENP exposures, the % DNA in tail was utilized as it is one of the most preferred parameters in comet assessments.[50] With the CometChip method, we were able to assess the induction of single-strand breakage in TK6 and H9T3 cells after exposure to three concentrations of a panel of five ENPs along with positive and negative controls simultaneously. Given the reduction in experimental noise that is associated with processing samples on a single chip, this approach contributes to the elucidation of subtle differences in DNA damage levels and is one of a few studies in which the genotoxicity of five industry relevant ENPs were evaluated concurrently.

Qualitative image data generated from the CometChip analysis of TK6 cells exposed to the ENP panel for 4 h are shown in Figure 2. Control or media-treated nucleoid structures show well-defined heads of undamaged DNA (Figure 2A) in comparison to ENP-exposed cells/nucleoids in Figure 2B with varying degrees of damage, whereas positive control cells exposed to a known DNA-damaging agent (hydrogen peroxide; 100 μM) revealed significant DNA damage (Figure 2C). TK6 cells exposed to zinc oxide nanoparticles and assayed using the traditional comet assay method for comparison are shown in Figure 2D. The qualitative data illustrated in Figure 2B were analyzed using custom MATLAB (The Mathworks) software in which the following quantitative assessments for each nanoparticle in TK6 cells (Figure 3A) in addition to H9T3 cells (Figure 3D) (qualitative data not shown). In addition to the CometChip analyses, we utilized the MTT and CyQuant NF to understand the affects of nanoparticle exposures on cellular viability and proliferation. The following observations were generated from the proposed ENP-mediated DNA damage screening platform and subsequent toxicity assays:

Cytotoxic and Genotoxic Influences of Amorphous Silica Exposures. The likelihood of human exposure to amorphous silica is extremely high, as exposures can stem from biogenic sources in addition to several nano-enabled consumer products that contain silica.[51] Amorphous silica ENPs were not anticipated to induce DNA damage at this dose range, based on previous studies.[52] Although here there does appear to be a slight increase in DNA damage induced by amorphous silica ENPs in each dose, the difference was not statistically significant compared to media alone ($p = 0.39$). It is worth noting that the results for Ag ENPs, which will be discussed in detail in the next section, appeared qualitatively similar and statistically significant in comparison to media control ($p = 0.0001$) (Figure 3A). Similar to our findings, reports of genotoxicity were found in HT29 cells exposed to mesoporous silica.[53] In contrast, negative genotoxicity results were found in a study evaluating multiple sizes of amorphous silica, ranging from 30 to 400 nm at 4 and 40 μg/mL on T3T-LI fibroblasts for 4 h.[54] Using the MTT assay, we found that amorphous silica nanoparticles imposed no reduction of metabolic activity in TK6 cells after 4 h exposure (Figure 3B), which correlates with similar studies using Balb/3T3 mouse fibroblasts in which no cytotoxicity nor genotoxicity was found after amorphous silica exposure.[52] Interestingly, a recent study revealed that amorphous silica toxicity is influenced by the doubling time of the cell, wherein normal cells that proliferate slower than the tumor cells tested had higher reduction in viability.[55] However, we found that amorphous silica nanoparticle

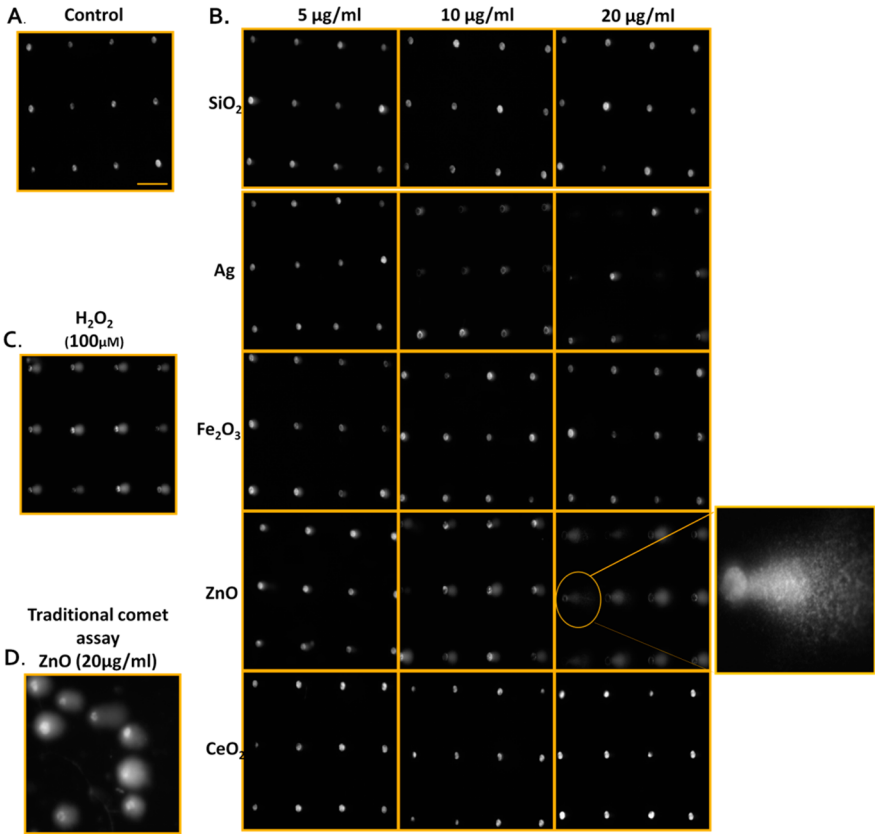

Figure 2. Qualitative images of nanoparticle-mediated ENP DNA damage in TK6 cells using both CometChip and standard comet assays. (A) Media-treated control cells. (B) TK6 cells were exposed to industrially relevant ENPs at concentrations of 5, 10, and 20 μg/mL for 4 h and evaluated using the CometChip technology. Expanded view illustrates the morphology of the comet structure induced from 4 h exposure of zinc oxide ENP in TK6, revealing significant DNA damage. (C) Positive control cells treated with H_2O_2 (100 μM) for 20 min. (D) Traditional comet assay of TK6 cells treated with ZnO (20 μg/mL) for 4 h for comparison to CometChip qualitative assessments. Horizontal scale bar represents 100 μm.

exposures did not alter TK6 cell proliferation after 4 h exposure (Figure 3C).

Although we determined amorphous silica ENPs to be nongenotoxic to H9T3 cells (Figure 3D), we did observe reduced cellular viability and proliferation after 24 h exposure at 10 and 20 μg/mL (Figure 3E,F). This coincides with several reports that amorphous silica can impose significant cellular toxicity.[56−58] Overall, amorphous silica is considered biologically inert in physiologically relevant doses, but the discrepancies in literature and our own study could be attributed to variations in particle preparation and dosimetry.

Silver ENPs Induce Single-Stranded DNA Damage and Reduction in Cellular Function. Silver ENPs have been incorporated into several personal hygiene and antimicrobial products and are the most commercialized nanomaterial.[59] More specifically, nanoenabled antimicrobial materials have been developed in the effort to combat several emerging or re-emerging drug-resistant bacteria by using silver nanoparticles.[60] However, alarmingly, several studies have determined their DNA damage potential in mammalian cells,[61] and our findings using the CometChip analysis are consistent with the published literature. Specifically, silver ENPs induced DNA damage in TK6 cells at each concentration (5, 10, 20 μg/mL) producing 16, 19, and 21% DNA in tail, respectively, which were statistically significant in comparison to media-only cells (8% DNA in tail) (Figure 3A). Previously, Asharani and co-workers utilized the traditional comet assay for DNA damage assessments of silver nanoparticle exposures in other cell types, namely, normal human fibroblasts and glioblastoma cells where dose-dependent increases in DNA damage were found.[62] Similar to other studies that identified reduction in cellular viability after exposure to silver, silver ENPs utilized in this study at the dose of 20 μg/mL exerted a significant reduction in viability (27%) in TK6 cells at 4 h post-exposure (Figure 3B). In regards to possible mechanism, Paio and co-workers demonstrated that silver nanoparticles were capable of disrupting mitochondrial membrane potential through a mitochondrial-dependent apoptotic pathway which is regulated by Bax and Bcl-2 genes. The dysregulation of these two genes created a cascade of events which eventually led to apoptosis in human liver cells.[63] Alternatively, a key mechanism for silver nanoparticle toxicity has been reported to be the reduction of mitochondrial function *via* inhibition of

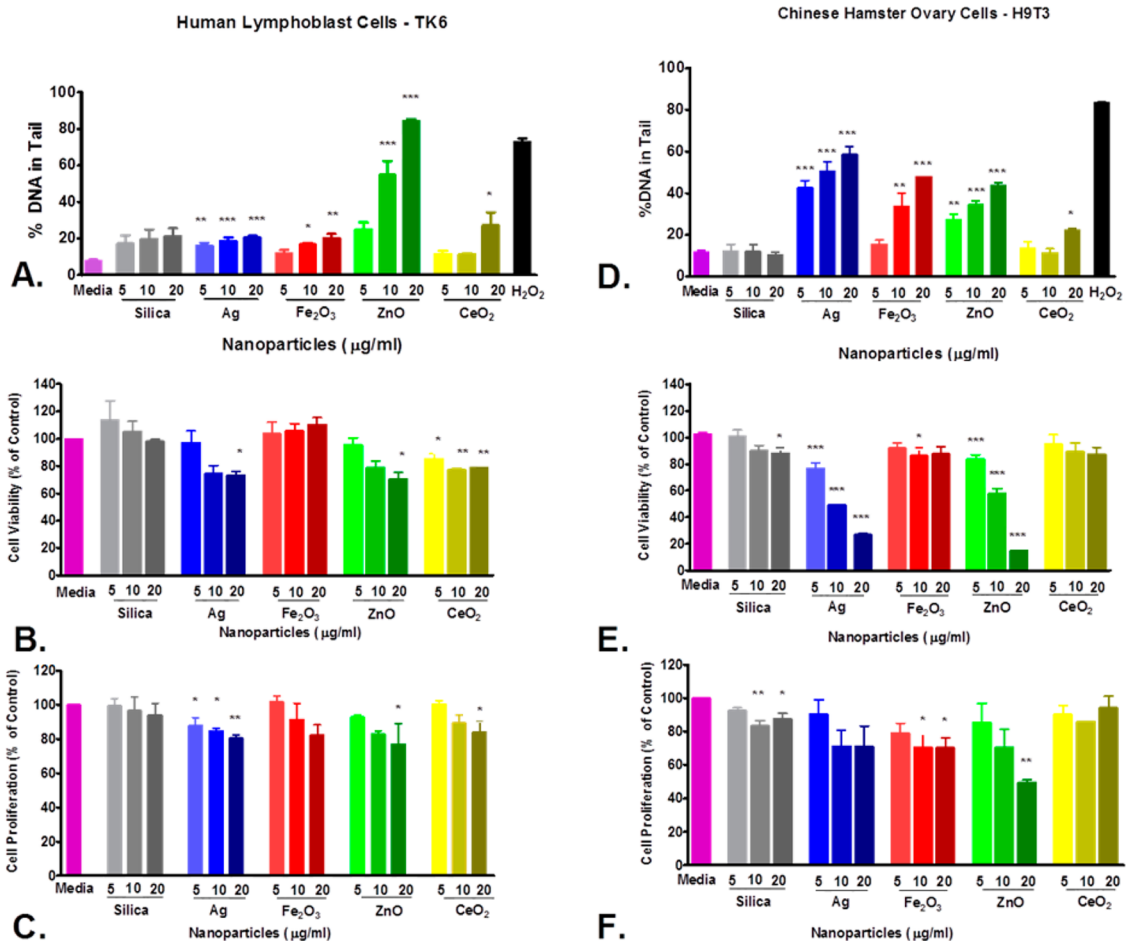

Figure 3. Evaluation of TK6 cells seeded at a density of 1×10^6 cells/well and H9T3 cells seeded at a density of 1×10^4 cells/well exposed to 5, 10, and 20 μg/mL of ENPs where (A,D) DNA damage, (B,E) cellular viability, and (C,F) CyQuant NF assessments were performed 4 and 24 h post-exposure, respectively. Data represent an average of three or more independent experiments performed in triplicate. The *p* values were determined by one-way ANOVA followed by Dunnett's post-test, where *$p \leq 0.05$, **$p \leq 0.01$, ***$p \leq 0.001$ *vs* media control.

ATP synthesis.[64] In reference to the proliferative effect of silver nanoparticles on TK6 cells, each dose imposed significant reductions in proliferation (Figure 3C). Although the effects of nanosilver on cellular function are not clearly understood, the concern over the use of silver ENPs in consumer products is warranted. In H9T3 cells, nanosilver elicited significant levels of DNA damage of 43, 51, and 59% DNA in tail for 5, 10, and 20 μg/mL doses, respectively at 24 h (Figure 3D). Silver ENP exposures were also capable of inducing significant reductions in H9T3 viability at 24 h post-exposure (Figure 3E). It is important to note that excessive cytotoxicity could introduce confounders within the genotoxicity assessments. However, the proliferative capacity of the utilized cells remained at acceptable levels at all concentrations of nanoparticles, which has been shown to be a more sensitive index of cytotoxicity in genotoxicity testing (Figure 3F).[65] These data are in agreement with the numerous reports of deleterious effects of nanosilver not only in mammalian cells but also in aquatic organisms.[66−68] The use of silver ENPs may have several benefits; however, understanding the risks are essential to ensure product safety and eliminate public and environmental health concerns.

Impact of Iron Oxide ENPs on DNA, Cellular Viability, and Proliferation. Currently, there is great interest in iron oxide ENPs, as their properties makes them useful in numerous applications such as biomedical imaging and possible tumor ablation therapies.[69] In the present study, iron oxide at 10 and 20 μg/mL resulted in 17 and 20% DNA in tail in TK6 cells after 4 h, respectively (Figure 3A). This finding correlates well with a recent study, in which nanoscale iron oxide (Fe_2O_3) significantly induced DNA damage in human lung cells,[70] which further calls into question the biocompatibility of this highly utilized nanomaterial.

While the interest and application of hematite continues to grow, conclusive evidence of its cytotoxicity is still under review. In our evaluations, we did not observe any reduction in cellular viability after hematite exposure for TK6 cells at 4 h (Figure 3B). Interestingly, there was a reduction in cell proliferation of 20% at 20 μg/mL (Figure 3C), which coincides with conflicting reports of hematite toxicity within the literature.[71]

The majority of this conflict is primarily due to differences in material preparation and particle size. For example, Freyia and co-workers found no relevant toxicity in mouse alveolar macrophages and human epithelial cells due to hematite exposures in the nano, submicrometer, and micrometer scale, thus suggesting that hematite regardless of size has little toxic effect.[71] In contrast, hematite *in vivo* exposures in nanoscale and submicrometer scale have been associated with lung injury.[72] Thus, iron nanoparticles may exhibit different biointeractions than micrometer-scale iron, but both could have deleterious effects to DNA, organelles, and biological processes.

Numerous model systems have been employed to investigate iron oxide nanoparticles and the potential novel toxicities they possess.[73−75] Using the CometChip platform, exposure to 10 and 20 μg/mL of Fe_2O_3 ENPs was found to be substantially genotoxic to H9T3 cells at 24 h with results of 33 and 48% DNA in tail (Figure 3D). These results differ from published findings on the genotoxicity of iron oxide, where no definitive genotoxic result was obtained from nano-sized or micrometer-sized hematite particle exposures in Syrian hamster embryo cells.[76] Karlsson and co-workers found similar negative results when evaluating hematite and magnetite nanoparticles.[77] Certain confounders such as cell type could be involved in conflicting reports of toxicity as particle uptake can be influenced by the cell phenotype.[78] Recent reports revealed that the redox state of hematite may also affect particle uptake and genotoxicity.[79] In addition to the single-stranded DNA damage observed in this study, hematite ENPs also reduced cellular viability in H9T3 cells by 14%; however, only 10 μg/mL elicited reductions that were statistically relevant (Figure 3E). Additionally, H9T3 cells displayed a significant 30% reduction in proliferation after iron oxide ENP exposures (Figure 3F). Thus, iron oxide is an attractive nanomaterial, due to its physicochemical properties and applications; however, those unique attributes may prove problematic in biological systems.

Zinc Oxide ENP Genotoxicity and Cytotoxicity. Zinc oxide ENPs are currently a main component in many sunscreen formulations due to its UVA and UVB absorptive properties.[80,81] However, several studies have correlated the exposure to zinc oxide nanoparticles to increased DNA damage, increased reactive oxygen species, and reduction in cell viability.[82,83] For the case of zinc oxide nanoparticle generated with our VENGES system, exposures at 10 and 20 μg/mL produced considerable injury, 55 and 84%, respectively, to DNA at 4 h in TK6 cells (Figure 3A). These findings are consistent with several studies that report the impact of zinc oxide nanoparticles.[84−87] For example, Alarifi and co-workers used low concentrations of zinc oxide nanoparticles (5, 10, 20 μg/mL) on malignant human melanoma skin cell line, A375, and found significant levels of genotoxicity using the standard comet assay along with chromosome condensation staining at 24 h in comparison to control.[88] From the data presented here, it is clear that zinc oxide ENPs can cause DNA damage; however, it is not clear if the observations can be attributed to the properties of the particles or ion dissolution.

Understanding the dissolution kinetics of partially soluble ENMs is important in assessing the genotoxic potential and toxicity mechanisms associated with both ionic and particulate components.[89] Recent studies have reported that only a few metal oxide nanoparticles are soluble in cell culture media, including ZnO and Ag investigated in this study.[90,91] For example, previous studies have demonstrated that reducing the solubility of ZnO particles leads to reduced cellular toxicity[92] and reduced inflammatory response when instilled in the rat lung.[93] The issue of dissolution becomes more complex considering the variety of intracellular microenvironments and pH conditions that will further influence solubility and intracellular particle trafficking.[94] Nevertheless, our data correlates with recent zinc oxide nanoparticle genotoxicity studies and confirm the hazardous nature of ZnO nanoparticles.[95,96]

Several studies also suggest that the release of Zn^{2+} ions from ZnO ENPs can damage other cellular organelles and their biological function.[91,97] Our MTT analysis revealed zinc oxide ENP exposure impaired mitochondrial dehydrogenase activity in TK6 by 26% at the high dose of 20 μg/mL (Figure 3B). These findings are similar to other studies that evaluated comparable concentrations of zinc oxide where the genotoxic effects were found at 3−6 h in SH-SY5Y cells.[98] The authors found that zinc oxide nanoparticles were more toxic to rapidly proliferating fibroblast cells due to increases in intracellular zinc concentrations.[98] In the present study, we observed similar trends *via* MTT and CyQuant NF analyses, where cellular viability inhibition was demonstrated as well as a considerable reduction in cellular proliferation by 23% after a 4 h exposure to zinc oxide ENPs in our suspension cell line, TK6 (Figure 3C).

In the adherent cell type, H9T3, we found significant levels of DNA damage due to zinc oxide ENP exposures of 34 and 44% DNA in tail for 10 and 20 μg/mL (Figure 3D). Additionally, zinc oxide ENP exposures significantly decreased cellular viability at the low dose of 5 μg/mL and drastically reduced H9T3 cells at 10 and 20 μg/mL, revealing 42 and 85% reduction in cell viability, respectively (Figure 3E). Zinc oxide nanoparticles impeded proliferation by 50% after 20 μg/mL in comparison to media only treated or control cells (Figure 3F), which correlates with our cellular viability and other studies which evaluated the toxicity of ZnO ENP exposures.[99−101] Clearly, the use of safer formulations of zinc ENP should be implemented in

nanoenabled products to reduce deleterious effects on biological systems.

Cerium Oxide ENP Exposure, DNA Damage, and the Cellular Effects. Cerium oxide is a known additive in many gasoline formulations, cosmetics, and a potential component in some disease therapies.[102] In regards to the genotoxic potential of CeO_2, we found that a dose of 20 μg/mL induced significant DNA damage (27%) (Figure 3A). Thought to be a radical scavenger,[103,104] cerium oxide's innate properties may act as a double-edged sword when taken up by cells. For example, Marzi and co-workers showed that, although cerium oxide ENPs could protect A549 and HepG2 cells from hydrogen-peroxide-mediated oxidative damage, the presence of cerium oxide ENPs alone could adversely affect cellular DNA.[105] Furthermore, normal human fibroblasts exposed to cerium ENPs incurred DNA damage after 2 h exposure in a separate study.[106] Conversely, a study conducted to evaluate the effects of cerium oxide on human lens epithelial cells found no induction of DNA damage after 24 h exposure.[107] Thus, the inherent properties of cerium may create complex interactions with DNA in certain cell populations. Although cerium oxide ENP exposures did not elicit a high amount of DNA damage, TK6 cells were still sensitive to low exposures of cerium oxide in which significant decreases in viability (15, 23, 21%) were found at 5, 10, and 20 μg/mL after 4 h exposure (Figure 3B). Hussain and co-workers found similar results when sublethal or low doses of cerium were used on human peripheral blood monocytes.[108] Within that study, the authors found extensive mitochondrial damage to cerium-exposed monocytes, including mitochondrial elongation, swelling, and depolarization, or decrease in membrane potential.[108] The authors suggested that cerium-mediated cytotoxicity was not associated with reactive oxygen species generation, which is the generally accepted cause of most metal oxide ENP toxicity.[108] Interestingly, there are limited reports about the adverse effects of cerium oxide nanoparticle exposures; in fact, many reports report their cytoprotective and proliferative nature.[109−111] However, in the present investigation, a reduction in TK6 cell proliferation (Figure 3C) by 16% was observed after 4 h exposure of cerium ENPs.

In regards to the genotoxicity of cerium oxide exposures in the adherent cell line, H9T3, significant DNA damage was found at 20 μg/mL (22% DNA in tail) (Figure 3D). However, cerium ENP exposures at 24 h did not interfere with cellular viability in H9T3 cells at higher concentrations (Figure 3E). Cerium ENP exposure at 20 μg/mL also did not reduce cellular proliferation in H9T3 cells after 24 h (Figure 3F), which correlates with cellular viability data mentioned previously. Therefore, in light of the complex nature of cerium oxide ENPs, future studies are warranted in order to retain the potential therapeutic benefits cerium may possess but minimize the health risks.

In summary, we have observed that the levels of DNA damage obtained using the presented CometChip approach covaried with diminished cell survival. For example, for zinc, in H9T3 cells, there was a dramatic decrease in viability at doses that are highly genotoxic according to the CometChip analysis. Silver and iron at the lower doses tested induced significant DNA damage, while retaining cell viability at levels 70−80% or higher. Generally, 70−80% viability is accepted as a level of cell death (determined by trypan blue dye exclusion assay) that does not interfere with the ability to assess DNA damage using the comet assay.[112] When using ATP levels or cell proliferation as a measure of cytotoxicity, cutoff levels of 50% viability or greater are recommended.[65,113] In regards to cerium oxide exposures, the highest concentration in H9T3 cells induced DNA damage but did not alter viability or cellular proliferation. In contrast, a significant decrease in cellular viability and proliferation was observed when TK6 cells incurred DNA damage due to cerium oxide ENP exposures. The variances in the correlation between cellular toxicity and genotoxicity are in agreement with reports in literature;[77,114,115] however, additional studies are warranted.

More importantly, the use of the CometChip platform revealed distinctive genotoxicity profiles for suspension (TK6) and adherent (H9T3) cell lines. The outcomes reported here are possibly due to cell-type-dependent differences in cell growth and adhesion, nanoparticle−cell interactions, and varying dosimetry over time. Recently, studies to investigate particle−cell interaction uncovered that not only was internalization size-dependent but the same material in different cell lines may display different uptake kinetics,[116] which could have implications on toxicity and ENP hazard ranking. However, to properly rank the hazards of the studied ENPs within and across cell lines, dosimetry needs to be taken into consideration to fully assess the toxicities observed. Although dosimetry or the measurement of the delivered dose is extremely important in this regard, rarely is it utilized in nanotoxicological studies.[117,118] This is primarily due to the fact that *in vitro* dosimetry is still an evolving field and well-accepted dosimetric tools are not readily available. Although our group has developed a dosimetry technique for adherent cell lines,[45] to the best of our knowledge, there is no published dosimetry method for suspension cells.[27] Thus, the presented DNA damage data presented here cannot be used for hazard ranking but could be used for the identification of genotoxic ENPs.

Another possible contributing factor in our observations is DNA repair. It is well-known that single-stranded DNA breaks are usually rapidly repaired in cells.[119] Thus, the genotoxicity profiles reported for the

H9T3 cell line, which were exposed for 24 h, could possibly be the result of repaired breaks and/or unrepaired breaks. Moreover, it is conceivable that genes associated with DNA damage response could be affected by the continued presence of ENPs within cells. For example, Petkovic and co-workers described the consequences of crystalline titanium in HepG2 cells and the deleterious downstream effects on DNA damage response genes, revealing their genotoxicity and ability to affect DNA repair.[120] Thus, all of these confounding factors could have contributed to the different ENP-induced DNA damage profiles reported within this study.

Although this approach has clear advantages over the traditional method in assessing DNA damage, there are some limitations. No single genotoxicity assay is perfect in its ability to detect the broad range of possible genetic changes that are potentially induced by environmental exposure.[121] Thus, regulators employ a range of genotoxicity tests, which generally include the Ames test (bacterial cell mutation), MN (*in vitro* micronucleus), and the TK (mammalian cell mutation) assays.[122] However, in the field of nanogenotoxicity, the comet assay has excelled past the previously mentioned methods due to its sensitivity.[123] Unlike the Ames and TK assays, the comet assay directly tests for DNA damage, as opposed to mutations that arise as a result of damage, offering an important advantage. Along the same line, a limitation of the comet assay is that the evaluation of comets does not allow discernment of the mechanism of action or mutagenic potential of test substances.[124] Recently, the incorporation of fluorescence *in situ* hybridization (FISH) or specific fluorophore-labeled DNA probes has enabled the simultaneous evaluation of damaged chromatin material and gene regions,[125,126] which could potentially provide insight into initial mutagenic/carcinogenic events caused by ENP exposure. Another limitation of the comet assay, which has proved problematic in generating reproducible results between different laboratories, is the lack of standardization in methodology, interpretation, and particle preparation.[54,127] Thus, the demonstrated CometChip protocol and platform could further the effort to provide harmonization for ENP genotoxicity assessments.

CONCLUSIONS

Here, we have demonstrated the efficacy of a high-throughput platform for assessing DNA damage in mammalian cells induced by ENP exposure. In addition to its high-throughput nature, the proposed CometChip approach has advantages over the traditional comet assay. The microfabricated cell array, 96-well plate format, and automated image processing reduces noise, bias, and labor but more importantly increases throughput by approximately two orders of magnitude compared to the traditional assay. We observed significant levels of single-stranded DNA damage in both TK6 and H9T3 cells, demonstrating the efficacy of this platform to produce robust sets of data to capture initial molecular events, which could be useful as a screening tool for various types of ENPs and potentially used for hazard ranking when dosimetry is considered.

We envision that the proposed approach will be not only an important tool for nanotoxicologists developing HT screening strategies for the assessment of possible adverse health effects associated with ENMs but also of great importance for material scientists working on the development of novel ENMs and safer-by-design approaches. For instance, the proposed CometChip approach was used in one of our recently published studies which focused on the development of a "safer-by-design" concept for ZnO NPs.[2] In this study, a safer-by-design concept was pursued by hermetically encapsulating ZnO nanorods in a biologically inert, nanothin amorphous SiO_2 coating during their gas-phase synthesis in an effort to maintain their optoelectronic properties and reduce at the same time the high DNA damage potential of ZnO NPs. The proposed CometChip approach was instrumental in this study to screen for DNA damage potential in the vast libraries of coated and uncoated ZnO NPs and derive the optimum nanoparticle/coating properties. This resulted in the development of SiO_2-coated ZnO nanorods with 3 times lower DNA damage potential compared to uncoated ZnO nanoparticles, rendering them attractive in polymers and cosmetics.

For future directions, we plan to expand the utility of the CometChip method to include the investigation of physiologically relevant cell lines, double-stranded DNA breaks, and specific DNA lesions using certain enzymes, which may be influenced by different nanomaterials. Moreover, with this tool, we can also probe for DNA damage in individual cells and in combination with fluorescent *in situ* hybridization and detect gene-specific regions, which may be altered or mutated by the presence of ENPs. The Comet–FISH technique has been utilized with great success in comparing the damage and repair of genes such as p53 and hTERT, thus providing a potential valuable method in clinical settings.[128]

Of greater importance, there is evidence that the *in vitro* comet assay can provide predictive information for *in vivo* genotoxic events induced by nanoparticle exposures. In a study performed by Ghosh and co-workers, good correlations were revealed between *in vitro* and *in vivo* silver nanoparticle (25 μg/mL)-mediated genotoxicity in cultured human blood lymphocytes and in Swiss albino male mice exposed to AgNPs *via* intraperitoneal injection (10 mg/kg) using the comet assay approach. Within that study, the authors also determined that silver nanoparticle exposures could fragment *Allium cepa* and *Nicotania tabacum* plant nuclear DNA using the comet assay when the plantlets were fed water containing Ag

nanomaterials for 24 h.[129] Thus, *in vitro* genotoxicity can be correlated to ENP-mediated DNA damage *in vivo* using the comet assay technique. Taken together, the CometChip method could prove to be a powerful tool in assessing DNA damage and possible gene mutations of ENPs, enhancing our ability to predict the consequences of ENP exposures *in vivo*. Current studies within our lab are underway to reveal the potential for predicting *in vivo* genotoxic outcomes using the CometChip platform.

METHODS

ENP Synthesis and Characterization in Powder Form. ENPs investigated in this study are listed in Table 1. ENP powders were generated in-house using the Harvard Versatile Engineered Nanomaterial Generation System (VENGES), as previously described.[40] Specific surface area, SSA, defined as the area per mass (m^2/g), was determined by the nitrogen adsorption/Brunauer–Emmett–Teller (BET) method (Monosorb by Quantachrome, Boynton Beach, FL). The equivalent primary particle diameter, d_{BET}, was calculated, assuming spherical particles, as

$$d_{BET} = \frac{6}{SSA \times \rho_P} \quad (1)$$

where ρ_P is the particle density, which was obtained for each particle from the densities of component materials, at 20 °C, reported in the CRC handbook of Chemistry and Physics.[130] Particle crystal size and diameter were also determined by X-ray diffraction using a Scintag XDS2000 powder diffractometer (Scintag Inc., Cupertino, CA), reported here as d_{XRD}. ENP powder primary particle morphology and size were further characterized by transmission electron microscopy (TEM) using a Zeiss Libra 120 microscope (Carl Zeiss GmbH, Jena, Germany).

ENP Dispersal and Characterization in Liquid Suspensions. Dispersions were prepared based on a protocol recently developed by the authors.[45] Sonication was performed in deionized water (DI H_2O) using the critical dispersion sonication energy (DSE_{cr}), which was determined as previously described for each ENP.[45] ENPs were dispersed at 1 mg/mL in 3 mL of solute in 15 mL conical polyethylene tubes using a Branson Sonifier S-450A (Branson Ultrasonics, Danbury, CT), calibrated by the calorimetric calibration method previously described,[45,131] whereby the power delivered to the sample was determined to be 1.25 W, fitted with a 3 in. cup horn (maximum power output of 400 W at 60 Hz, continuous mode, output level 3) in which tubes were immersed so that sample and cup water menisci were aligned. Stock DI H_2O suspensions were then diluted to final desired concentrations (5, 10, or 20 μg/mL) in RPMI 1640 or MEM cell culture media, each either alone or supplemented with 10% heat-inactivated horse serum (HS) or fetal bovine serum (FBS), respectively, 100 U/mL penicillin, and 100 μg/mL streptomycin and vortexed for 30 s. Dispersions were analyzed for hydrodynamic diameter (d_H), polydispersity index (PDI), zeta-potential (ζ), and specific conductance (σ) by DLS using a Zetasizer Nano-ZS (Malvern Instruments, Worcestershire, UK).

Cell Culture and Treatment. TK6 human lymphoblastoid and H9T3 Chinese hamster ovary cell lines were kind gifts from Bevin Engelward of Massachusetts Institute of Technology. TK6 cells were maintained in RPMI-1640 with L-glutamine supplemented with 10% horse serum and 100 units/mL penicillin and streptomycin. H9T3 cells were cultivated in minimum essential media (MEM) with 10% fetal bovine serum and 100 units/mL penicillin and streptomycin. Both cell lines were utilized for experimentation at passage 13. Cells were seeded at a density of 2×10^5 cells/well in a 96-well plate in 100 μL approximately 1 h before treatment for TK6 cells. H9T3 cells were plated at a density of 1×10^4cells/well 1 day prior to nanoparticle treatment and allowed to reach confluency before treatment. Nanoparticle suspensions were prepared and sonicated as mentioned in Figure 1 in 3 mg/mL concentrated stocks in sterile distilled water. The stocks were then diluted in the appropriate media containing 10% serum and adjusted to the correct concentration. Each suspension was vortexed prior to adding to the cell suspension at a volume of 100 μL for 4 h for TK6 cells and 24 h for H9T3 cells. We utilized longer exposure times for H9T3 cells to ensure nanoparticle/cell interaction.

CometChip Preparation and Cell Loading. Negative silicon molds of polydimethylsiloxane (PDMS) were used to pattern microwells within the 96-well platform as described by Wood *et al.* and Weingeist *et al.*[36,37] The PDMS mold was allowed to set in molten 1% normal melting point agarose applied to GelBond film for 20 min. After agarose polymerization, the PDMS stamp was removed, revealing a 300 μm thick gel consisting of arrayed microwells. The gel was then clamped between a bottomless 96-well plate and a glass plate. Cells which were pre-exposed with ENPs for 3.5 h were then added to the microwell array and allowed to load for 30 min for a total 4 h exposure. In regards to H9T3 cells, after 23 h of ENP exposure, spent medium was aspirated and cell monolayers were washed with 1× phosphate buffered saline (PBS). Cells were then trypsinized with 50 μL of TrypLE reagent for 4 min. Complete media containing 10% fetal bovine serum (50 μL) were added to wells to deactivate trypsin. The treated cell suspensions were then transferred to the CometChip for 30 min to 1 h. After gravitational settling of cells into single wells, excess cells were aspirated and the gel was rinsed three times with warm 1× PBS. Molten low melting 1% agarose was used to cover microwell array/cells and allowed to set for 5 min at room temperature and 5 min at 4 °C. The gel was then submerged into lysis solution (2.5 M NaCl, 100 mM Na_2EDTA, 10 mM Tris, pH 9.5 with 0.5% Triton X-100) overnight at 4 °C. After lysis, gels were washed two times in PBS to remove surfactant. Gels were then adhered to an electrophoresis inner tank well (Trevigen) with double-sided tape gel side up. Electrophoresis was performed using alkaline buffer (0.3 M sodium hydroxide and 1 mM Na_2EDTA in distilled water) at 4 °C for 30 min at 21 V and 300 mA. After neutralization with 0.4 M Tris-HCl buffer, Sybrgold (Invitrogen) stain was used to detect fragmented DNA within microwells at a concentration of 1:2000 in 1× TBE buffer.

Traditional Comet Assay. To prove the efficacy and efficiency of the CometChip, comparison studies were performed using the traditional comet assay. Briefly, TK6 cells which were exposed to ZnO (20 μg/mL) for 4 h were submerged in 1% molten agarose and placed on glass slides. The molten agarose/cell mixture was allowed to set and subsequently placed into lysis solution (2.5 M NaCl, 100 mM Na_2EDTA, 10 mM Tris, pH 9.5 with 0.5% Triton X-100) for 1 h at 4 °C. After lysis, exposed nucleoid structures were placed in alkaline solution to allow unwinding. Slides were then electrophoresed using alkaline buffer (0.3 M sodium hydroxide and 1 mM Na_2EDTA in distilled water) at 4 °C for 30 min at 21 V and 300 mA. Sybrgold stain (1:1000) was used to stain damaged DNA, and an Axiovert inverted fluorescent microscope was employed for imaging.

Cellular Viability Evaluation. The MTT assay (Roche) was used to assess the cell viability of TK6 and H9T3 cells exposed to nanoparticles. TK6 cells, a suspension lymphoblastoid cell line, were seeded into 96-well plates at a density of 1×10^4 cells/well in RPMI media in 100 μL containing 10% horse serum. Nanoparticle suspensions were added at 100 μL at twice the concentration needed to obtain 5, 10, and 20 μg/mL for 4 h at 37 °C in 5% CO_2. After exposure, cells were spun down at 250*g*, and spent medium was aspirated. Fresh medium was then added, and MTT reagent (3-[4,5-dimethylthiazol-2-yl]-2,5-diphenyl tetrazolium bromide) (10 μL) was added to each well for a period of 4 h at 37 °C. Solubilization reagent (100 μL) was added to dissolve the formazan crystals produced from the reduction of the tetrazolium salt or MTT reagent in viable cells. Absorbance was measured at 550 nm using a fluorescence microplate reader (Molecular Devices). Acellular experiments were performed to

ensure reagent integrity and to rule out ENP interference. The data obtained from acellular experiments revealed no interaction between test ENPs and MTT reagents during the 4 h exposure time point in TK6 cells. For the 24 h time point utilized in the H9T3 cells, no substantial nanoparticle interaction with MTT reagents was observed. Percent cell viability (relative viability compared to media-only cells) was calculated as mean value ± standard error as a result of three independent experiments performed in triplicate.

Cellular Proliferation Assay. To measure cellular proliferation after nanoparticle exposure, the CyQuant NF assay was employed. Independent of metabolic function, this assay utilizes the amount of DNA in correlation to cellular proliferation. Briefly, cells were seeded in black 96-well plates at a density of 1×10^4 cells/well in the appropriate culture media containing 10% horse serum or 5% fetal bovine serum at a volume of 100 μL for TK6 and H9T3 cells, respectively. Nanoparticle suspensions were added to the cell suspensions at twice the concentration desired and incubated for 4 h at 37 °C at 5% CO_2. After exposure, plates containing cell and nanoparticle suspensions were spun down at 250*g*, and medium was aspirated. CyQuant NF dye reagent diluted in 1× HBSS (Hank's balanced salt solution) buffer (100 μL) was added to cells and incubated for 30 min at 37 °C. Negative controls were cells without nanoparticle suspensions. Background autofluorescence of TK6 and H9T3 cells from unstained cells were measured in addition to negative controls. To account for possible nanoparticle interference with reagents, plates with ENPs only were performed simultaneously. The ENP-only plates reflected slight background noise and thus were subtracted from data collected from ENP/cell proliferation evaluation. Fluorescence measurements were taken immediately using a microplate reader (Molecular Devices) at an excitation of 485 nm and emission detection of 530 nm. All experiments were performed in triplicate for a total number of three experiments. Values reported are the mean ± standard error. One-way ANOVA was performed followed by Dunnett's post test; *p* values less than 0.05 were considered significant.

Statistical Analysis. Experimental investigations were conducted three times, and results were expressed as means ± SEM for at least three biological experiments. Statistical differences between the means were determined by performing one-way analysis of variance (ANOVA) using Prism version 5 (GraphPad Software, La Jolla, CA), and a treatment effect with a *p* value of ≤0.05 was considered significant. Individual groups for comet analysis were compared using the unpaired Dunnett's post test.

Chemicals and Reagents. All chemicals and reagents to synthesize metal nanoparticles used within this study were purchased from Sigma Aldrich. RPMI-1640 and minimal essential media (MEM) cell culture media, penicillin/streptomycin, horse serum, and GelBond film were purchased from Lonza. Low and high melting agarose plus all electrophoresis reagents and buffers were purchased from Sigma Aldrich. MTT cellular viability assay was purchased from Roche, and cell proliferation CyQuant NF assay was acquired from Invitrogen.

Conflict of Interest: The authors declare no competing financial interest.

Acknowledgment. We kindly acknowledge the financial support from the National Science Foundation (grant no. 1235806) and NIH (grant no. P30ES000002). C.W. is funded by the NIH NHLBI Ruth L. Kirschstein T32 training grant (NIH HL007118). Additionally, we would like to thank J. Brain for his mentorship and R. Molina for his insightful commentary. This work was performed in part at the Harvard Center for Nanoscale Systems (CNS), a member of the National Nanotechnology Infrastructure Network (NNIN), which is supported by the National Science Foundation under NSF award no. ECS-0335765.

Supporting Information Available: TEM figures cited in the text as Figure S1. This material is available free of charge *via* the Internet at http://pubs.acs.org.

REFERENCES AND NOTES

1. Woodrow Wilson International Center for Scholars—Project on Emerging Nanotechnologies; http://www.nanotechproject.org/inventories/consumer/.
2. Sotiriou, G.; Watson, C.; Murdaugh, K.; Darrah, T.; Pyrgiotakis, P.; Elder, A.; Brain, J.; Demokritou, P. Engineering Safer-by-Design, Transparent, Silica-Coated ZnO Nanorods with Reduced DNA Damage Potential. *Environ. Sci.: Nano.* **2014**, 10.1039/C3EN00062A.
3. Bello, D.; Martin, J.; Santeufemio, C.; Sun, Q.; Lee Bunker, K.; Shafer, M.; Demokritou, P. Physicochemical and Morphological Characterisation of Nanoparticles from Photocopiers: Implications for Environmental Health. *Nanotoxicology* **2012**, 989–1003.
4. Maynard, A. D.; Warheit, D. B.; Philbert, M. A. The New Toxicology of Sophisticated Materials: Nanotoxicology and Beyond. *Toxicol. Sci.* **2011**, *120*, S109–S129.
5. Pirela, S.; Molina, R.; Watson, C.; Cohen, J.; Bello, D.; Demokritou, P.; Brain, J. Effects of Copy Center Particles on the Lungs: A Toxicological Characterization Using a Balb/C Mice Model. *Inhal. Toxicol.* **2013**, 498–508.
6. Zhao, J.; Castranova, V. Toxicology of Nanomaterials Used in Medicine. *J. Toxicol. Environ. Health, Part B* **2011**, *14*, 593–632.
7. Kuhlbusch, T.; Asbach, C.; Fissan, H.; Gohler, D.; Stintz, M. Nanoparticle Exposure at Nanotechnology Workplaces: A Review. *Part. Fibre Toxicol.* **2011**, *8*, 22.
8. Wan, R.; Mo, Y.; Feng, L.; Chien, S.; Tollerud, D. J.; Zhang, Q. DNA Damage Caused by Metal Nanoparticles: Involvement of Oxidative Stress and Activation of ATM. *Chem. Res. Toxicol.* **2012**, *25*, 1402–1411.
9. Oberdörster, G.; Maynard, A.; Donaldson, K.; Castranova, V.; Fitzpatrick, J.; Ausman, K.; Carter, J.; Karn, B.; Kreyling, W.; Lai, D.; *et al.* Principles for Characterizing the Potential Human Health Effects from Exposure to Nanomaterials: Elements of a Screening Strategy. *Part. Fibre Toxicol.* **2005**, *2*, 8.
10. Demokritou, P.; Gass, S.; Pyrgiotakis, G.; Cohen, J. M.; Goldsmith, W.; McKinney, W.; Frazer, D.; Ma, J.; Schwegler-Berry, D.; Brain, J.; *et al.* An *In Vivo* and *In Vitro* Toxicological Characterisation of Realistic Nanoscale CeO_2 Inhalation Exposures. *Nanotoxicology* **2012**, *7*, 1338–1350.
11. Madl, A.; Pinkerton, K. E. Health Effects of Inhaled Engineered and Incidental Nanoparticles. *Crit. Rev. Toxicol.* **2009**, *39*, 629–658.
12. Simko, M.; Mattsson, M. O. Risks from Accidental Exposures to Engineered Nanoparticles and Neurological Health Effects: A Critical Review. *Part. Fibre Toxicol.* **2010**, *7*, 42.
13. Song, M. F.; Li, Y. S.; Kasai, H.; Kawai, K. Metal Nanoparticle-Induced Micronuclei and Oxidative DNA Damage in Mice. *J. Clin. Biochem. Nutr.* **2012**, *50*, 211–216.
14. Valko, M.; Rhodes, C. J.; Moncol, J.; Izakovic, M.; Mazur, M. Free Radicals, Metals and Antioxidants in Oxidative Stress-Induced Cancer. *Chem. Biol. Interact.* **2006**, *160*, 1–40.
15. Jomova, K.; Valko, M. Advances in Metal-Induced Oxidative Stress and Human Disease. *Toxicology* **2011**, *283*, 65–87.
16. Dizdaroglu, M. Oxidatively Induced DNA Damage: Mechanisms, Repair and Disease. *Cancer Lett.* **2012**, *327*, 26–47.
17. Paschos, A.; Pandya, R.; Duivenvoorden, W. C.; Pinthus, J. H. Oxidative Stress in Prostate Cancer: Changing Research Concepts towards a Novel Paradigm for Prevention and Therapeutics. *Prostate Cancer Prostatic Dis.* **2013**, 217–225.
18. Helleday, T.; Lo, J.; van Gent, D. C.; Engelward, B. P. DNA Double-Strand Break Repair: From Mechanistic Understanding to Cancer Treatment. *DNA Repair* **2007**, *6*, 923–935.
19. Li, Y.; Chen, D.; Yan, J.; Chen, Y.; Mittelstaedt, R. A.; Zhang, Y.; Biris, A. S.; Heflich, R. H.; Chen, T. Genotoxicity of Silver Nanoparticles Evaluated Using the Ames Test and *In Vitro* Micronucleus Assay. *Mutat. Res., Genet. Toxicol. Environ. Mutagen.* **2012**, *745*, 4–10.
20. Singh, N.; Manshian, B.; Jenkins-Gareth, J. S.; Griffiths, S. M.; Williams, P. M.; Maffeis, T. G. G.; Wright, C. J.; Doak,

S. H. Nanogenotoxicology: The DNA Damaging Potential of Engineered Nanomaterials. *Biomaterials* **2009**, *30*, 3891–3914.
21. Landsiedel, R.; Kapp, M. D.; Schulz, M.; Wiench, K.; Oesch, F. Genotoxicity Investigations on Nanomaterials: Methods, Preparation and Characterization of Test Material, Potential Artifacts and Limitations—Many Questions, Some Answers. *Mutat. Res.* **2009**, *681*, 241–258.
22. Kazimirova, A.; Magdolenova, Z.; Barancokova, M.; Staruchova, M.; Volkovova, K.; Dusinska, M. Genotoxicity Testing of PLGA-PEO Nanoparticles in TK6 Cells by the Comet Assay and the Cytokinesis-Block Micronucleus Assay. *Mutat. Res.* **2012**, *748*, 42–47.
23. Jiang, X.; Foldbjerg, R.; Miclaus, T.; Wang, L.; Singh, R.; Hayashi, Y.; Sutherland, D.; Chen, C.; Autrup, H.; Beer, C. Multi-platform Genotoxicity Analysis of Silver Nanoparticles in the Model Cell Line Cho-K1. *Toxicol. Lett.* **2013**, *222*, 55–63.
24. Kumar, A.; Sharma, V.; Dhawan, A. Methods for Detection of Oxidative Stress and Genotoxicity of Engineered Nanoparticles. *Methods Mol. Biol.* **2013**, *1028*, 231–246.
25. Singh, S. P.; Rahman, M. F.; Murty, U. S.; Mahboob, M.; Grover, P. Comparative Study of Genotoxicity and Tissue Distribution of Nano and Micron Sized Iron Oxide in Rats after Acute Oral Treatment. *Toxicol. Appl. Pharmacol.* **2013**, *266*, 56–66.
26. Magdolenova, Z.; Collins, A.; Kumar, A.; Dhawan, A.; Stone, V.; Dusinska, M. Mechanisms of Genotoxicity: A Review of *In Vitro* and *In Vivo* Studies with Engineered Nanoparticles. *Nanotoxicology* **2013**, *8*, 233–278.
27. Doak, S. H.; Griffiths, S. M.; Manshian, B.; Singh, N.; Williams, P. M.; Brown, A. P.; Jenkins, G. J. S. Confounding Experimental Considerations in Nanogenotoxicology. *Mutagenesis* **2009**, *24*, 285–293.
28. Ma, P.; Luo, Q.; Chen, J.; Gan, Y.; Du, J.; Ding, S.; Xi, Z.; Yang, X. Intraperitoneal Injection of Magnetic Fe_3O_4-Nanoparticle Induces Hepatic and Renal Tissue Injury *via* Oxidative Stress in Mice. *Int. J. Nanomed.* **2012**, *7*, 4809–4818.
29. Karlsson, H. L. The Comet Assay in Nanotoxicology Research. *Anal. Bioanal. Chem.* **2010**, *398*, 651–666.
30. Ostling, O.; Johanson, K. J. Microelectrophoretic Study of Radiation-Induced DNA Damages in Individual Mammalian Cells. *Biochem. Biophys. Res. Commun.* **1984**, *123*, 291–298.
31. Singh, N. P.; McCoy, M. T.; Tice, R. R.; Schneider, E. L. A Simple Technique for Quantitation of Low Levels of DNA Damage in Individual Cells. *Exp. Cell Res.* **1988**, *175*, 184–191.
32. Stone, V.; Johnston, H.; Schins, R. P. Development of *In Vitro* Systems for Nanotoxicology: Methodological Considerations. *Crit. Rev. Toxicol.* **2009**, *39*, 613–626.
33. Magdolenova, Z.; Lorenzo, Y.; Collins, A.; Dusinska, M. Can Standard Genotoxicity Tests Be Applied to Nanoparticles? *J. Toxicol. Environ. Health, Part A* **2012**, *75*, 800–806.
34. García, O.; Mandina, T.; Lamadrid, A. I.; Diaz, A.; Remigio, A.; Gonzalez, Y.; Piloto, J.; Gonzalez, J. E.; Alvarez, A. Sensitivity and Variability of Visual Scoring in the Comet Assay. Results of an Inter-Laboratory Scoring Exercise with the Use of Silver Staining. *Mutat. Res.* **2004**, *556*, 25–34.
35. Arora, S.; Rajwade, J. M.; Paknikar, K. M. Nanotoxicology and *In Vitro* Studies: The Need of the Hour. *Toxicol. Appl. Pharmacol.* **2012**, *258*, 151–165.
36. Wood, D. K.; Weingeist, D. M.; Bhatia, S. N.; Engelward, B. P. Single Cell Trapping and DNA Damage Analysis Using Microwell Arrays. *Proc. Natl. Acad. Sci. U.S.A.* **2010**, *107*, 10008–10013.
37. Weingeist, D. M.; Ge, J.; Wood, D. K.; Mutamba, J. T.; Huang, Q.; Rowland, E. A.; Yaffe, M. B.; Floyd, S.; Engelward, B. P. Single-Cell Microarray Enables High-Throughput Evaluation of DNA Double-Strand Breaks and DNA Repair Inhibitors. *Cell Cycle* **2013**, *12*, 907–915.
38. Nel, A.; Xia, T.; Meng, H.; Wang, X.; Lin, S.; Ji, Z.; Zhang, H. Nanomaterial Toxicity Testing in the 21st Century: Use of a Predictive Toxicological Approach and High-Throughput Screening. *Acc. Chem. Res.* **2012**, *46*, 607–621.
39. Preliminary Guidance Notes on Sample Preparation and Dosimetry for the Safety Testing of Manufactured Nanomaterials. *OECD*, **2010**.
40. Demokritou, P. Development and Characterization of a Versatile Engineered Nanomaterial Generation System (VENGES) Suitable for Toxicological Studies. *Inhal. Toxicol.* **2010**, *22*, 2107–2116.
41. Sotiriou, G. A.; Diaz, E.; Long, M. S.; Godleski, J.; Brain, J.; Pratsinis, S. E.; Demokritou, P. A Novel Platform for Pulmonary and Cardiovascular Toxicological Characterization of Inhaled Engineered Nanomaterials. *Nanotoxicology* **2012**, *6*, 680–690.
42. Gass, S.; Cohen, J. M.; Pyrgiotakis, G.; Sotiriou, G. A.; Pratsinis, S. E.; Demokritou, P. A Safer Formulation Concept for Flame-Generated Engineered Nanomaterials. *ACS Sustainable Chem. Eng.* **2013**, *1*, 843–857.
43. Raming, T. P.; Winnubst, A. J.; Van Kats, C. M.; Philipse, A. P. The Synthesis and Magnetic Properties of Nanosized Hematite (α-Fe_2O_3) Particles. *J. Colloid Interface Sci.* **2002**, *249*, 346–350.
44. Amin, N.; Arajs, S. Morin Temperature of Annealed Submicronic α-F_2O_3 Particles. *Phys. Rev. B: Condens. Matter Mater. Phys.* **1987**, *35*, 4810–4811.
45. Cohen, J.; Deloid, G.; Pyrgiotakis, G.; Demokritou, P. Interactions of Engineered Nanomaterials in Physiological Media and Implications for *In Vitro* Dosimetry. *Nanotoxicology* **2013**, *7*, 417–431.
46. Møller, P.; Möller, L.; Godschalk, R. W. L.; Jones, G. D. D. Assessment and Reduction of Comet Assay Variation in Relation to DNA Damage: Studies from the European Comet Assay Validation Group. *Mutagenesis* **2010**, *25*, 109–111.
47. Azqueta, A.; Collins, A. R. The Essential Comet Assay: A Comprehensive Guide To Measuring DNA Damage and Repair. *Arch. Toxicol.* **2013**, *87*, 949–968.
48. Kimura, A.; Miyata, A.; Honma, M. A Combination of *In Vitro* Comet Assay and Micronucleus Test Using Human Lymphoblastoid TK6 Cells. *Mutagenesis* **2013**, *28*, 583–590.
49. Bajpayee, M.; Kumar, A.; Dhawan, A. The Comet Assay: Assessment of *In Vitro* and *In Vivo* DNA Damage. *Methods Mol. Biol.* **2013**, *1044*, 325–345.
50. Collins, A. R.; Oscoz, A. A.; Brunborg, G.; Gaivao, I.; Giovannelli, L.; Kruszewski, M.; Smith, C. C.; Stetina, R. The Comet Assay: Topical Issues. *Mutagenesis* **2008**, *23*, 143–151.
51. Fruijtier-Polloth, C. The Toxicological Mode of Action and the Safety of Synthetic Amorphous Silica—A Nanostructured Material. *Toxicology* **2012**, *294*, 61–79.
52. Uboldi, C.; Giudetti, G.; Broggi, F.; Gilliland, D.; Ponti, J.; Rossi, F. Amorphous Silica Nanoparticles Do Not Induce Cytotoxicity, Cell Transformation or Genotoxicity in Balb/3t3 Mouse Fibroblasts. *Mutat. Res.* **2012**, *745*, 11–20.
53. Sergent, J. A.; Paget, V.; Chevillard, S. Toxicity and Genotoxicity of Nano-SiO_2 on Human Epithelial Intestinal Ht-29 Cell Line. *Ann. Occup. Hyg.* **2012**, *56*, 622–630.
54. Barnes, C.; Elsaesser, A.; Arkusz, J.; Smok, A.; Palus, J.; Leśniak, A.; Salvati, A.; Hanrahan, J. P.; Jong, W. H.; Dziubałtowska, E.; *et al.* Reproducible Comet Assay of Amorphous Silica Nanoparticles Detects No Genotoxicity. *Nano Lett.* **2008**, *8*, 3069–3074.
55. Chang, J.; Chang, K. L.; Hwang, D. F.; Kong, Z. L. *In Vitro* Cytotoxicitiy of Silica Nanoparticles at High Concentrations Strongly Depends on the Metabolic Activity Type of the Cell Line. *Environ. Sci. Technol.* **2007**, *41*, 2064–2068.
56. Napierska, D.; Thomassen, L. C.; Lison, D.; Martens, J. A.; Hoet, P. H. The Nanosilica Hazard: Another Variable Entity. *Part. Fibre Toxicol.* **2010**, *7*, 39.
57. Ahamed, M. Silica Nanoparticles-Induced Cytotoxicity, Oxidative Stress and Apoptosis in Cultured A431 and A549 Cells. *Hum. Exp. Toxicol.* **2013**, *32*, 186–195.
58. Guidi, P.; Nigro, M.; Bernardeschi, M.; Scarcelli, V.; Lucchesi, P.; Onida, B.; Mortera, R.; Frenzilli, G. Genotoxicity of

Amorphous Silica Particles with Different Structure and Dimension in Human and Murine Cell Lines. *Mutagenesis* **2013**, *28*, 171–180.
59. De Jong, W. H.; Van Der Ven, L. T.; Sleijffers, A.; Park, M. V.; Jansen, E. H.; Van Loveren, H.; Vandebriel, R. J. Systemic and Immunotoxicity of Silver Nanoparticles in an Intravenous 28 Days Repeated Dose Toxicity Study in Rats. *Biomaterials* **2013**, *34*, 8333–8343.
60. Rai, M. K.; Deshmukh, S. D.; Ingle, A. P.; Gade, A. K. Silver Nanoparticles: The Powerful Nanoweapon against Multidrug-Resistant Bacteria. *J. Appl. Microbiol.* **2012**, *112*, 841–852.
61. Kim, S.; Ryu, D. Y. Silver Nanoparticle-Induced Oxidative Stress, Genotoxicity and Apoptosis in Cultured Cells and Animal Tissues. *J. Appl. Toxicol.* **2013**, *33*, 78–89.
62. AshaRani, P. V.; Low Kah, M. G.; Hande, M. P.; Valiyaveettil, S. Cytotoxicity and Genotoxicity of Silver Nanoparticles in Human Cells. *ACS Nano* **2008**, *3*, 279–290.
63. Piao, M. J.; Kang, K. A.; Lee, I. K.; Kim, H. S.; Kim, S.; Choi, J. Y.; Choi, J.; Hyun, J. W. Silver Nanoparticles Induce Oxidative Cell Damage in Human Liver Cells through Inhibition of Reduced Glutathione and Induction of Mitochondria-Involved Apoptosis. *Toxicol. Lett.* **2011**, *201*, 92–100.
64. Asare, N.; Instanes, C.; Sandberg, W. J.; Refsnes, M.; Schwarze, P.; Kruszewski, M.; Brunborg, G. Cytotoxic and Genotoxic Effects of Silver Nanoparticles in Testicular Cells. *Toxicology* **2012**, *291*, 65–72.
65. O'Donovan, M. A Critique of Methods To Measure Cytotoxicity in Mammalian Cell Genotoxicity Assays. *Mutagenesis* **2012**, *27*, 615–621.
66. Massarsky, A.; Dupuis, L.; Taylor, J.; Eisa-Beygi, S.; Strek, L.; Trudeau, V. L.; Moon, T. W. Assessment of Nanosilver Toxicity during Zebrafish (*Danio rerio*) Development. *Chemosphere* **2013**, *92*, 59–66.
67. Powers, C. M.; Slotkin, T. A.; Seidler, F. J.; Badireddy, A. R.; Padilla, S. Silver Nanoparticles Alter Zebrafish Development and Larval Behavior: Distinct Roles for Particle Size, Coating and Composition. *Neurotoxicol. Teratol.* **2011**, *33*, 708–714.
68. Kwok, K. W.; Auffan, M.; Badireddy, A. R.; Nelson, C. M.; Wiesner, M. R.; Chilkoti, A.; Liu, J.; Marinakos, S. M.; Hinton, D. E. Uptake of Silver Nanoparticles and Toxicity to Early Life Stages of Japanese Medaka (*Oryzias latipes*): Effect of Coating Materials. *Aquat. Toxicol.* **2012**, *120−121*, 59–66.
69. Laurent, S.; Mahmoudi, M. Superparamagnetic Iron Oxide Nanoparticles: Promises for Diagnosis and Treatment of Cancer. *Int. J. Mol. Epidemiol. Genet.* **2011**, 2.
70. Bhattacharya, K.; Hoffmann, E.; Schins, R. F.; Boertz, J.; Prantl, E. M.; Alink, G. M.; Byrne, H. J.; Kuhlbusch, T. A.; Rahman, Q.; Wiggers, H.; *et al.* Comparison of Micro- and Nanoscale Fe^{+3}-Containing (Hematite) Particles for Their Toxicological Properties in Human Lung Cells *in Vitro*. *Toxicol. Sci.* **2012**, *126*, 173–182.
71. Freyria, F. S.; Bonelli, B.; Tomatis, M.; Ghiazza, M.; Gazzano, E.; Ghigo, D.; Garrone, E.; Fubini, B. Hematite Nanoparticles Larger than 90 nm Show No Sign of Toxicity in Terms of Lactate Dehydrogenase Release, Nitric Oxide Generation, Apoptosis, and Comet Assay in Murine Alveolar Macrophages and Human Lung Epithelial Cells. *Chem. Res. Toxicol.* **2012**, *25*, 850–861.
72. Zhu, M. T.; Feng, W. Y.; Wang, B.; Wang, T. C.; Gu, Y. Q.; Wang, M.; Wang, Y.; Ouyang, H.; Zhao, Y. L.; Chai, Z. F. Comparative Study of Pulmonary Responses to Nano- and Submicron-Sized Ferric Oxide in Rats. *Toxicology* **2008**, *247*, 102–111.
73. Kalive, M.; Zhang, W.; Chen, Y.; Capco, D. G. Human Intestinal Epithelial Cells Exhibit a Cellular Response Indicating a Potential Toxicity upon Exposure to Hematite Nanoparticles. *Cell Biol. Toxicol.* **2012**, *28*, 343–368.
74. Zhang, W.; Kalive, M.; Capco, D. G.; Chen, Y. Adsorption of Hematite Nanoparticles onto Caco-2 Cells and the Cellular Impairments: Effect of Particle Size. *Nanotechnology* **2010**, *21*, 355103.
75. Zhang, W.; Hughes, J.; Chen, Y. Impacts of Hematite Nanoparticle Exposure on Biomechanical, Adhesive, and Surface Electrical Properties of *Escherichia coli* Cells. *Appl. Environ. Microbiol.* **2012**, *78*, 3905–3915.
76. Guichard, Y.; Schmit, J.; Darne, C.; Gate, L.; Goutet, M.; Rousset, D.; Rastoix, O.; Wrobel, R.; Witschger, O.; Martin, A.; *et al.* Cytotoxicity and Genotoxicity of Nanosized and Microsized Titanium Dioxide and Iron Oxide Particles in Syrian Hamster Embryo Cells. *Ann. Occup. Hyg.* **2012**, *56*, 631–644.
77. Karlsson, H. L.; Gustafsson, J.; Cronholm, P.; Möller, L. Size-Dependent Toxicity of Metal Oxide Particles—A Comparison between Nano- and Micrometer Size. *Toxicol. Lett.* **2009**, *188*, 112–118.
78. Kemp, S. J.; Thorley, A. J.; Gorelik, J.; Seckl, M. J.; O'Hare, M. J.; Arcaro, A.; Korchev, Y.; Goldstraw, P.; Tetley, T. D. Immortalization of Human Alveolar Epithelial Cells To Investigate Nanoparticle Uptake. *Am. J. Respir. Cell Mol. Biol.* **2008**, *39*, 591–597.
79. Singh, N.; Jenkins, G. J. S.; Nelson, B. C.; Marquis, B. J.; Maffeis, T. G. G.; Brown, A. P.; Williams, P. M.; Wright, C. J.; Doak, S. H. The Role of Iron Redox State in the Genotoxicity of Ultrafine Superparamagnetic Iron Oxide Nanoparticles. *Biomaterials* **2012**, *33*, 163–170.
80. Nohynek, G. J.; Lademann, J.; Ribaud, C.; Roberts, M. S. Grey Goo on the Skin? Nanotechnology, Cosmetic and Sunscreen Safety. *Crit. Rev. Toxicol.* **2007**, *37*, 251–277.
81. Monteiro-Riviere, N. A.; Wiench, K.; Landsiedel, R.; Schulte, S.; Inman, A. O.; Riviere, J. E. Safety Evaluation of Sunscreen Formulations Containing Titanium Dioxide and Zinc Oxide Nanoparticles in UVB Sunburned Skin: An *In Vitro* and *In Vivo* Study. *Toxicol. Sci.* **2011**, *123*, 264–280.
82. Sharma, V.; Anderson, D.; Dhawan, A. Zinc Oxide Nanoparticles Induce Oxidative Stress and Genotoxicity in Human Liver Cells (HepG2). *J. Biomed. Nanotechnol.* **2011**, *7*, 98–99.
83. Valdiglesias, V.; Costa, C.; Kilic, G.; Costa, S.; Pasaro, E.; Laffon, B.; Teixeira, J. P. Neuronal Cytotoxicity and Genotoxicity Induced by Zinc Oxide Nanoparticles. *Environ. Int.* **2013**, *55*, 92–100.
84. Wilhelmi, V.; Fischer, U.; Weighardt, H.; Schulze-Osthoff, K.; Nickel, C.; Stahlmecke, B.; Kuhlbusch, T. A.; Scherbart, A. M.; Esser, C.; Schins, R. P.; *et al.* Zinc Oxide Nanoparticles Induce Necrosis and Apoptosis in Macrophages in a P47 Phox- and Nrf2-Independent Manner. *PLoS One* **2013**, *8*, e65704.
85. Fukui, H.; Horie, M.; Endoh, S.; Kato, H.; Fujita, K.; Nishio, K.; Komaba, L. K.; Maru, J.; Miyauhi, A.; Nakamura, A.; *et al.* Association of Zinc Ion Release and Oxidative Stress Induced by Intratracheal Instillation of ZnO Nanoparticles to Rat Lung. *Chem. Biol. Interact.* **2012**, *198*, 29–37.
86. Deng, X.; Luan, Q.; Chen, W.; Wang, Y.; Wu, M.; Zhang, H.; Jiao, Z. Nanosized Zinc Oxide Particles Induce Neural Stem Cell Apoptosis. *Nanotechnology* **2009**, *20*, 115101.
87. Hsiao, I. L.; Huang, Y. J. Effects of Serum on Cytotoxicity of Nano- and Micro-sized ZnO Particles. *J. Nanopart. Res.* **2013**, *15*, 1829.
88. Alarifi, S.; Ali, D.; Alkahtani, S.; Verma, A.; Ahmed, M.; Alhadlaq, H. A. Induction of Oxidative Stress, DNA Damage, and Apoptosis in a Malignant Human Skin Melanoma Cell Line after Exposure to Zinc Oxide Nanoparticles. *Int. J. Nanomed.* **2013**, *8*, 983–993.
89. Franklin, N. M.; Rogers, N. J.; Apte, S. C.; Batley, G. E.; Gadd, G. E.; Casey, P. S. Comparative Toxicity of Nanoparticulate ZnO, Bulk ZnO, and $ZnCl_2$ to a Freshwater Microalga (*Pseudokirchneriella subcapitata*): The Importance of Particle Solubility. *Environ. Sci. Technol.* **2007**, *41*, 8484–8490.
90. James, S. A.; Feltis, B. N.; de Jonge, M. D.; Sridhar, M.; Kimpton, J. A.; Altissimo, M.; Mayo, S.; Zheng, C.; Hastings, A.; Howard, D. L.; *et al.* Quantification of ZnO Nanoparticle Uptake, Distribution, and Dissolution within Individual Human Macrophages. *ACS Nano* **2013**, *7*, 10621–10635.

91. Kao, Y. Y.; Chen, Y. C.; Cheng, T. J.; Chiung, Y. M.; Liu, P. S. Zinc Oxide Nanoparticles Interfere with Zinc Ion Homeostasis To Cause Cytotoxicity. *Toxicol. Sci.* **2012**, *125*, 462–472.
92. Hsiao, I. L.; Huang, Y. J. Titanium Oxide Shell Coatings Decrease the Cytotoxicity of ZnO Nanoparticles. *Chem. Res. Toxicol.* **2011**, *24*, 303–313.
93. Xia, T.; Zhao, Y.; Sager, T.; George, S.; Pokhrel, S.; Li, N.; Schoenfeld, D.; Meng, H.; Lin, S.; Wang, X.; *et al.* Decreased Dissolution of ZnO by Iron Doping Yields Nanoparticles with Reduced Toxicity in the Rodent Lung and Zebrafish Embryos. *ACS Nano* **2011**, *5*, 1223–1235.
94. Muller, K. H.; Kulkarni, J.; Motskin, M.; Goode, A.; Winship, P.; Skepper, J. N.; Ryan, M. P.; Porter, A. E. pH-Dependent Toxicity of High Aspect Ratio ZnO Nanowires in Macrophages Due to Intracellular Dissolution. *ACS Nano* **2010**, *4*, 6767–6779.
95. Guan, R.; Kang, T.; Lu, F.; Zhang, Z.; Shen, H.; Liu, M. Cytotoxicity, Oxidative Stress, and Genotoxicity in Human Hepatocyte and Embryonic Kidney Cells Exposed to ZnO Nanoparticles. *Nanoscale Res. Lett.* **2012**, *7*, 602.
96. Vandebriel, R. J.; De Jong, W. H. A Review of Mammalian Toxicity of ZnO Nanoparticles. *Nanotechnol. Sci. Appl.* **2012**, *5*, 61–71.
97. Song, W.; Zhang, J.; Guo, J.; Zhang, J.; Ding, F.; Li, L.; Sun, Z. Role of the Dissolved Zinc Ion and Reactive Oxygen Species in Cytotoxicity of ZnO Nanoparticles. *Toxicol. Lett.* **2010**, *199*, 389–397.
98. Taccola, L.; Raffa, V.; Riggio, C.; Vittorio, O.; Iorio, M. C.; Vanacore, R.; Pietrabissa, A.; Cuschieri, A. Zinc Oxide Nanoparticles as Selective Killers of Proliferating Cells. *Int. J. Nanomed.* **2011**, *6*, 1129–1140.
99. Dufour, E. K.; Kumaravel, T.; Nohynek, G. J.; Kirkland, D.; Toutain, H. Clastogenicity, Photo-clastogenicity or Pseudo-photo-clastogenicity: Genotoxic Effects of Zinc Oxide in the Dark, in Pre-irradiated or Simultaneously Irradiated Chinese Hamster Ovary Cells. *Mutat. Res., Genet. Toxicol. Environ. Mutagen.* **2006**, *607*, 215–224.
100. Ahamed, M.; Akhtar, M. J.; Raja, M.; Ahmad, I.; Siddiqui, M. K.; AlSalhi, M. S.; Alrokayan, S. A. ZnO Nanorod-Induced Apoptosis in Human Alveolar Adenocarcinoma Cells *via* P53, Survivin and Bax/Bcl-2 Pathways: Role of Oxidative Stress. *Nanomedicine* **2011**, *7*, 904–913.
101. Sayes, C. M.; Reed, K. L.; Warheit, D. B. Assessing Toxicity of Fine and Nanoparticles: Comparing *In Vitro* Measurements to *In Vivo* Pulmonary Toxicity Profiles. *Toxicol. Sci.* **2007**, *97*, 163–180.
102. Wason, M. S.; Zhao, J. Cerium Oxide Nanoparticles: Potential Applications for Cancer and Other Diseases. *Am. J. Transl. Res.* **2013**, *5*, 126–131.
103. Lord, M. S.; Jung, M.; Teoh, W. Y.; Gunawan, C.; Vassie, J. A.; Amal, R.; Whitelock, J. M. Cellular Uptake and Reactive Oxygen Species Modulation of Cerium Oxide Nanoparticles in Human Monocyte Cell Line U937. *Biomaterials* **2012**, *33*, 7915–7924.
104. Dowding, J. M.; Dosani, T.; Kumar, A.; Seal, S.; Self, W. T. Cerium Oxide Nanoparticles Scavenge Nitric Oxide Radical (NO). *Chem. Commun.* **2012**, *48*, 4896–4898.
105. Marzi, L. D.; Monaco, A.; De Lapuente, J.; Ramos, D.; Borras, M.; Di Gioacchino, M.; Santucci, S.; Poma, A. Cytotoxicity and Genotoxicity of Ceria Nanoparticles on Different Cell Lines *in Vitro*. *Int. J. Mol. Sci.* **2013**, *14*, 3065–3077.
106. Auffan, M.; Rose, J.; Orsiere, T.; De Meo, M.; Thill, A.; Zeyons, O.; Proux, O.; Masion, A.; Chaurand, P.; Spalla, O.; *et al.* CeO_2 Nanoparticles Induce DNA Damage towards Human Dermal Fibroblasts *in Vitro*. *Nanotoxicology* **2009**, *3*, 161–171.
107. Pierscionek, B. K.; Li, Y.; Yasseen, A. A.; Colhoun, L. M.; Schachar, R. A.; Chen, W. Nanoceria Have No Genotoxic Effect on Human Lens Epithelial Cells. *Nanotechnology* **2010**, *21*, 035102.
108. Hussain, S.; Al-Nsour, F.; Rice, A. B.; Marshburn, J.; Yingling, B.; Ji, Z.; Zink, J. I.; Walker, N. J.; Garantziotis, S. Cerium Dioxide Nanoparticles Induce Apoptosis and Autophagy in Human Peripheral Blood Monocytes. *ACS Nano* **2012**, *6*, 5820–5829.
109. Chigurupati, S.; Mughal, M. R.; Okun, E.; Das, S.; Kumar, A.; McCaffery, M.; Seal, S.; Mattson, M. P. Effects of Cerium Oxide Nanoparticles on the Growth of Keratinocytes, Fibroblasts and Vascular Endothelial Cells in Cutaneous Wound Healing. *Biomaterials* **2013**, *34*, 2194–2201.
110. Hosseini, A.; Baeeri, M.; Rahimifard, M.; Navaei-Nigjeh, M.; Mohammadirad, A.; Pourkhalili, N.; Hassani, S.; Kamali, M.; Abdollahi, M. Antiapoptotic Effects of Cerium Oxide and Yttrium Oxide Nanoparticles in Isolated Rat Pancreatic Islets. *Hum. Exp. Toxicol.* **2013**, *32*, 544–553.
111. Ciofani, G.; Genchi, G. G.; Liakos, I.; Cappello, V.; Gemmi, M.; Athanassiou, A.; Mazzolai, B.; Mattoli, V. Effects of Cerium Oxide Nanoparticles on Pc12 Neuronal-like Cells: Proliferation, Differentiation, and Dopamine Secretion. *Pharm. Res.* **2013**, *30*, 2133–2145.
112. Tice, R. R.; Agurell, E.; Anderson, D.; Burlinson, B.; Hartmann, A.; Kobayashi, H.; Miyamae, Y.; Rojas, E.; Ryu, J. C.; Sasaki, Y. F. Single Cell Gel/Comet Assay: Guidelines for *In Vitro* and *In Vivo* Genetic Toxicology Testing. *Environ. Mol. Mutagen.* **2000**, *35*, 206–221.
113. Kiskinis, E.; Suter, W.; Hartmann, A. High Throughput Comet Assay Using 96-Well Plates. *Mutagenesis* **2002**, *17*, 37–43.
114. Hong, S. C.; Lee, J. H.; Lee, J.; Kim, H. Y.; Park, J. Y.; Cho, J.; Lee, J.; Han, D. W. Subtle Cytotoxicity and Genotoxicity Differences in Superparamagnetic Iron Oxide Nanoparticles Coated with Various Functional Groups. *Int. J. Nanomed.* **2011**, *6*, 3219–3231.
115. Broggi, F.; Pontil, J.; Giudetti, G.; Franchini, F.; Stone, V.; Pascual García, C.; Rossi, F. Silver Nanoparticles Induce Cytotoxicity, but Not Cell Transformation or Genotoxicity on Balb3t3 Mouse Fibroblasts. *BioNanoMaterials* **2013**, *14*, 49–60.
116. dos Santos, T.; Varela, J.; Lynch, I.; Salvati, A.; Dawson, K. A. Quantitative Assessment of the Comparative Nanoparticle-Uptake Efficiency of a Range of Cell Lines. *Small* **2011**, *7*, 3341–3349.
117. Teeguarden, J. G.; Hinderliter, P. M.; Orr, G.; Thrall, B. D.; Pounds, J. G. Particokinetics *in Vitro*: Dosimetry Considerations for *In Vitro* Nanoparticle Toxicity Assessments. *Toxicol. Sci.* **2007**, *95*, 300–312.
118. Hinderliter, P. M.; Minard, K. R.; Orr, G.; Chrisler, W. B.; Thrall, B. D.; Pounds, J. G.; Teeguarden, J. G. ISDD: A Computational Model of Particle Sedimentation, Diffusion and Target Cell Dosimetry for *In Vitro* Toxicity Studies. *Part. Fibre Toxicol.* **2010**, *7*, 36.
119. Caldecott, K. W. Single-Strand Break Repair and Genetic Disease. *Nat. Rev. Genet.* **2008**, *9*, 619–631.
120. Petkovic, J.; Zegura, B.; Stevanovic, M.; Drnovsek, N.; Uskokovic, D.; Novak, S.; Filipic, M. DNA Damage and Alterations in Expression of DNA Damage Responsive Genes Induced by TiO_2 Nanoparticles in Human Hepatoma HepG2 Cells. *Nanotoxicology* **2011**, *5*, 341–353.
121. Sasaki, Y. F.; Sekihashi, K.; Izumiyama, F.; Nishidate, E.; Saga, A.; Ishida, K.; Tsuda, S. The Comet Assay with Multiple Mouse Organs: Comparison of Comet Assay Results and Carcinogenicity with 208 Chemicals Selected from the Iarc Monographs and U.S. Ntp Carcinogenicity Database**. *Crit. Rev. Toxicol.* **2000**, *30*, 629–799.
122. Kirkland, D. J.; Henderson, L.; Marzin, D.; Muller, L.; Parry, J. M.; Speit, G.; Tweats, D. J.; Williams, G. M. Testing Strategies in Mutagenicity and Genetic Toxicology: An Appraisal of the Guidelines of the European Scientific Committee for Cosmetics and Non-Food Products for the Evaluation of Hair Dyes. *Mutat. Res.* **2005**, *588*, 88–105.
123. Kim, H. R.; Park, Y. J.; Shin, D. Y.; Oh, S. M.; Chung, K. H. Appropriate *In Vitro* Methods for Genotoxicity Testing of Silver Nanoparticles. *Environ. Health Toxicol.* **2013**, *28*, e2013003.
124. Brendler-Schwaab, S.; Hartmann, A.; Pfuhler, S.; Speit, G. The *In Vivo* Comet Assay: Use and Status in Genotoxicity Testing. *Mutagenesis* **2005**, *20*, 245–254.

125. Horváthová, E.; Dušinská, M.; Shaposhnikov, S.; Collins, A. R. DNA Damage and Repair Measured in Different Genomic Regions Using the Comet Assay with Fluorescent *In Situ* Hybridization. *Mutagenesis* **2004**, *19*, 269–276.
126. Shaposhnikov, S.; Frengen, E.; Collins, A. R. Increasing the Resolution of the Comet Assay Using Fluorescent *In Situ* Hybridization—A Review. *Mutagenesis* **2009**, *24*, 383–389.
127. Walmsley, R. M.; Billinton, N. How Accurate Is *In Vitro* Prediction of Carcinogenicity? *Br. J. Pharmacol.* **2011**, *162*, 1250–1258.
128. McKenna, D. J.; Doherty, B. A.; Downes, C. S.; McKeown, S. R.; McKelvey-Martin, V. J. Use of the Comet-FISH Assay To Compare DNA Damage and Repair in P53 and hTERT Genes Following Ionizing Radiation. *PLoS One* **2012**, *7*, e49364.
129. Ghosh, M.; J, M.; Sinha, S.; Chakraborty, A.; Mallick, S. K.; Bandyopadhyay, M.; Mukherjee, A. *In Vitro* and *In Vivo* Genotoxicity of Silver Nanoparticles. *Mutat. Res.* **2012**, *749*, 60–69.
130. Haynes, W. M. *CRC Handbook of Chemistry and Physics*; CRC Press/Taylor and Francis: Boca Raton, FL, 2011.
131. Taurozzi, J. S.; Hackley, V. A.; Wiesner, M. R. Ultrasonic Dispersion of Nanoparticles for Environmental, Health and Safety Assessment: Issues and Recommendations. *Nanotoxicology* **2011**, *5*, 711–729.